Nutrition 63–64 (2019) 126–133

Contents lists available at ScienceDirect

Nutrition

journal homepage: www.nutritionjrnl.com

Basic nutritional investigation

Metformin treatment affects adipocytokine secretion and lipid composition in adipose tissues of diet-induced insulin-resistant rats

Sławomir Grycel Ph.D. [a], Adam R. Markowski Ph.D. [b], Hady Razak Hady Ph.D. [c], Piotr Zabielski Ph.D. [d,e], Iwona Kojta M.Sc. [f], Monika Imierska M.Sc. [f], Jan Górski Ph.D. [e,g], Agnieszka U. Blachnio-Zabielska Ph.D. [e,*]

[a] *Specialist Medical Center "SOMED" Łomża, Poland*
[b] *Department of Internal Medicine and Gastroenterology, Polish Red Cross Memorial Municipal Hospital, Bialystok, Poland*
[c] *1st Department of General Surgery and Endocrinology, Medical University Bialystok, Bialystok, Poland*
[d] *Department of Medical Biology, Medical University of Bialystok, Bialystok, Poland*
[e] *Department of Physiology, Medical University of Bialystok, Bialystok, Poland*
[f] *Department of Hygiene, Epidemiology and Metabolic Disorders, Medical University of Bialystok, Bialystok, Poland*
[g] *Department of Basic Sciences, Faculty of Health Sciences, Lomza State University of Applied Sciences, Lomza, Poland*

ARTICLE INFO

Article History:
Received 21 October 2018
Received in revised form 9 January 2019
Accepted 25 January 2019

Keywords:
Insulin resistance
Visceral adipose tissue
Subcutaneous adipose tissue
Metformin
Ceramide
DAG
Mass spectrometry

ABSTRACT

Objectives: Adipose tissue plays a central role in the pathogenesis of insulin resistance (IR) and type 2 diabetes. However, the molecular changes that promote these diseases are not completely understood. Several studies demonstrated that ceramide (Cer) and diacylglycerol (DAG) accumulation in muscle is associated with IR. The aim of this study was to explain whether a high-fat diet (HFD) leads to bioactive lipid accumulation in adipose tissue and how metformin affects the lipid content in adipocytes and the concentration of plasma adipocytokines.
Methods: The experiments were conducted on male Wistar rats divided into three groups: control, HFD-fed, and HFD-fed and treated with metformin. Cer and DAGs were analyzed by liquid chromatography tandem mass spectrometry. Phosphorylation of hormone-sensitive lipase (HSL) was analyzed by Western blot. Oral glucose tolerance and insulin tolerance tests were also performed. Plasma adiponectin and tumor necrosis factor (TNF)-α concentration were measured by enzyme-linked immunosorbent assay.
Results: HFD induced IR and elevated DAGs and Cer content in subcutaneous and visceral adipose tissues, which was accompanied by an increased phosphorylation of HSL. Metformin improved insulin sensitivity, decreased Cer and DAG levels, and attenuated the phosphorylation of HSL in both fat depots. Furthermore, we observed a strong correlation between adiponectin (negative) and TNF-α (positive) and bioactive lipids in both fat tissues.
Conclusions: These results indicated that bioactive lipids accumulation in adipose tissue influences the induction of IR and, at least in part, answered the question of what the insulin-sensitizing effect of metformin at the level of adipose tissue is.

Introduction

Adipose tissue plays a central role in the pathogenesis of insulin resistance (IR) associated with obesity. The main role of adipose tissue is to store energy in the form of triacylglycerols (TGs). However, more recently, the attention has been focused on the endocrine function of adipose tissue. Often, it has been demonstrated that adipocytokines secreted by adipose tissue affect insulin sensitivity of other peripheral tissues, such as skeletal muscles and liver [1,2]. These factors include leptin, adiponectin, tumor necrosis factor (TNF)-α, interleukin (IL)-6, and plasminogen activator inhibitor (PAI)-1 [3–5]. Fat tissue is located in numerous places on an organism, and different fat depots have distinct metabolic activity and, in an uneven way, contribute to the formation of metabolic disorders. Over the years, studies have strengthened the notion that obesity is not a homogeneous condition and that the regional fat distribution is an important indicator for metabolic alterations [6–8]. Epidemiologic studies have shown a strong correlation

This work was supported by the Foundation for Polish Science Grant HOMING PLUS/2010-2/1. PZ performed statistical analysis. ABZ designed the experiments and wrote and edited the manuscript. All authors participated in the data collection and reviewed the manuscript. The authors have no conflicts of interest to declare.

* Corresponding author: Tel.: +48 85686 52 26; Fax: +48 85 748 5560.
E-mail address: Agnieszka.blachnio@umb.edu.pl (A.U. Blachnio-Zabielska).

https://doi.org/10.1016/j.nut.2019.01.019
0899-9007/

between abdominal obesity and metabolic syndrome. The epidemic of abdominal obesity has drawn attention to visceral adipose tissue (VAT) as a risk factor for type 2 diabetes (T2D22DD) and other metabolic disorders associated with obesity. Both, subcutaneous adipose tissue (SAT) and visceral fat are characterized by production and secretion of a unique profile of adipocytokines. In the VAT, higher concentrations of IL-6 and PAI-1 were observed, whereas in the SAT, a higher level of leptin and adiponectin were noticed [9]. Moreover, compared with subcutaneous depot, VAT is a metabolically very active tissue and fulfills an important role as a source of circulating fatty acids (FAs). Free fatty acids (FFAs) are much more easily liberated from visceral fat than from subcutaneous fat. Under physiologic conditions, insulin inhibits the activity of the hormone-sensitive lipase (HSL), so in the presence of high glucose concentration, the release of FAs is limited. IR of adipose tissue is manifested mainly by the impaired ability to inhibit HSL by insulin, which results in an increased plasma FFA concentration despite high glucose levels. Once the FAs are liberated, they are taken up by other peripheral tissues (e.g., skeletal muscle) where they are used as a source of energy in the β-oxidation process or as a substrate for de novo synthesis of other lipids. Several lines of evidence suggest that accumulation of intramuscular lipids is responsible for induction of IR in skeletal muscles [10,11]. Among these lipids are ceramides (Cer) and diacylglycerols (DAG). Initially, it has been demonstrated that the accumulation of these lipids in muscle inhibits the insulin pathway and therefore glucose cannot be effectively taken up by this tissue [12–14]. A growing body of evidence implicates the contribution of these lipids to the induction of IR also in the liver [15–18]. Much less is known about the effect of Cer and DAG accumulation in adipose tissue. To our knowledge, there are only few papers indicating the relationship between the accumulation of these lipids and IR [19–24]. The existing data show that the Cer content is higher in the SAT of obese men and women than in lean non-diabetic individuals [20]. Another study, where biologically active lipids were examined in SAT and epicardial adipose tissue (EAT), demonstrated that the Cer content is higher in both SAT and EAT of obese people regardless of whether they have diabetes. In addition, a positive correlation has been shown between C16:0-Cer and homeostatic model assessment (HOMA)-IR and between HOMA-IR and C16:0/18:2 DAG in SAT [21]. Although adipose tissue appears to play a key role in the induction of IR, there are no specifically designed antidiabetic drugs targeted for adipose tissue. The first-line treatment for IR or T2D is metformin. This medication belongs to biguanide that are derived from *Galega officinalis*, used in herbal medicine. Metformin is thought to act mainly on the liver where it reduces hepatic glucose production. There is very limited information about metformin action in adipose tissue. Available data indicate that metformin activates AMP kinase (AMPK), which in turn catalyzes the phosphorylation of HSL at the inhibitory site (Ser-565), thus inhibiting the activity of this enzyme, which leads to a reduction in the release of FAs [25,26]. Metformin treatment has been defined as an effective therapy, but the detailed mechanism underlying its activities is complex and still remains incompletely understood. To our knowledge, there are no works presenting the effect of metformin treatment on the bioactive lipids content in adipose tissue. Because adipose tissue plays a central role in induction of IR and biologically active lipids affect the insulin action in other tissues, it seems important to study the role of lipid accumulation in fat tissue on insulin sensitivity and how metformin affects the content of these lipids, HSL activity, and adipocytokine secretion. Therefore, the present study was conducted to examine the effect of a high-fat diet (HFD) on the content of Cer and DAG in visceral and subcutaneous fat tissues. Moreover, we tried to understand how metformin treatment affects the content of the lipids in both adipose tissues. We also aimed to determine if there is any relationship between active lipids in adipose tissues and IR parameters or between individual lipid species and adiponectin or TNF-α levels.

Research design and methods

Animals and study design

The study was approved by the Institutional Animal Care and Use Committee of Medical University of Bialystok. All animal experiments were performed in accordance with the relevant guidelines and regulations. The experiments were carried out on male Wistar rats, 6 to 7 wk of age (140–150 g initial body weight) housed in standard conditions (21 ± 2°C, 12-h light/12-h dark cycle) with free access to tap water and food pellets. Animals were randomly divided into following groups (n = 8 in each group):

- Group 1: Control group, fed ad libitum a control diet (Research Diets INC D12450 B).
- Group 2: Fed the HFD (Research Diets INC D12492).
- Group 3: Fed the HFD but in week 5, oral metformin (300 mg/kg daily) was introduced, and the HFD and metformin treatment was continued for the next 3 wk.

The control diet contained 10% kcal from fat; whereas the HFD contained 60% kcal from fat. All groups were fed for 8 wk with the appropriate diet. Plasma insulin and glucose concentration were checked weekly for HOMA-IR calculation (to estimate the time for metformin introduction). One day before sacrifice, an insulin tolerance test (ITT) and an oral glucose tolerance test (OGTT) were performed. Thirty min before sacrifice, insulin (0.5 U/kg) was administered by intraperitoneal injection. The rats were anesthetized by intraperitoneal injection of pentobarbital at a dose of 80 mg/kg of body weight. The fat tissue from two depots (visceral fat from around the liver and subcutaneous fat from the abdomen region) was taken and frozen in liquid nitrogen and then stored at −80°C until analysis.

Lipid measurements

Plasma FFA concentration was measured by liquid chromatography tandem mass spectrometry (LC/MS) according to Persson et al. [27]. FAs were separated on a reverse-phase Zorbax SB-C18 column 2.1 × 150 mm, 1.8 μm using binary gradient. Buffer A was 80% acetonitrile, 0.5 mM ammonium acetate; buffer B was 99% acetonitrile, 1% 0.5 mM ammonium acetate.

Cer content in both fat depots was analyzed with the use of an ultra-high performance (UHP)LC MS/MS approach according to Blachnio-Zabielska et al. [28] with minor modification. Briefly, the adipose tissue samples (~20 mg) were pulverized in liquid nitrogen and then homogenized in a solution composed of 0.25 M sucrose, 25 mM KCl, 50 mM Tris, and 0.5 mM EDTA, pH 7.4. Immediately afterward, the internal standard [d17:1/8:0, d17:1/18:0, d17:1/18:1(9 Z), d17:1/20:0, d17:1/24:0 and d17:1/24:1(15 Z), Avanti Polar Lipids, Alabaster, AL, USA] and extraction mixture (isopropanol to water to ethyl acetate, 30:10:60; v:v:v) were added to each homogenate. The mixture was vortexed, sonicated, and then centrifuged for 10 min at 4000*g* (Sorvall Legend RT). The supernatant was transferred to a new tube and pellet was reextracted. Supernatants were combined and evaporated under nitrogen. The dried sample was reconstituted in 100 μL of LC Solvent A (2 mM ammonium formate, 0.15% formic acid in methanol) for LC/MS/MS analysis. Measurements were made using triple quadrupole MS operated in positive ion electrospray ionization (ESI) with multiple reaction monitoring (MRM). Concentration of each compound was analyzed against the concentration standard curves.

The content of DAG was measured using a UHPLC/MS/MS approach according to Blachnio-Zabielska et al. [29]. DAGs were extracted together with sphingolipids. A known amount of internal standard mix (Deuterated DAG Mixture I and Mixture II, Avanti Polar Lipids) was added to each sample. Next, samples were extracted as described earlier. The following DAG species were quantified: C18:1/18:2, C16:0/18:2, C16:0/16:0, C16:0/18:1, C18:0/20:0, C18:0/18:1, C18:1/18:1, C18:0/18:2 and C16:0/18:0 using UHPLC/MS/MS. DAG content was analyzed by means of a triple quadrupole MS using positive ion electrospray ionization source with MRM against the concentration standard curves.

Western blot

Fat tissue samples were homogenized in radioimmunoprecipitation buffer. After centrifugation and separation of fat cake, soluble proteins were precipitated with ice-cold methanol or chloroform, and protein pellets were suspended and denaturized in Laemmli buffer. Equal amounts of protein (20 mg in Laemmli buffer) were separated by 10% sodium dodecyl sulfate-polyacrylamide gel electrophoresis. Separated proteins were transferred on polyvinylidene fluoride membranes (Bio-Rad). The membrane was probed with an appropriate primary

antibody. The following target proteins were quantified: HSL (ab45422 in concentration 0.5 μg/mL, Abcam, Cambridge, UK), pHSL (Ser563) (Cell Signaling [4139] in concentration of 0.2 μg/mL) and pHSL (Ser660) (Cell Signaling [4126] in concentration of 0.2 μg/mL). Bands were visualized with the use of appropriate horseradish peroxidase-conjugated secondary antibodies and BioRad ChemiDoc XRS+ imager. Values were normalized to GAPDH (ab181602, used at 0.05 μg/mL, Abcam) protein expression measured from parallel runs and expressed as fold-changes over control group values. Unless stated otherwise, all chemicals and equipment used for immunoblotting were purchased from Bio-Rad (Hercules, CA, USA). The Image Lab 6.0 software was used for blot analysis.

Plasma adiponectin and TNF-α concentration

The plasma adiponectin and TNF-α concentration were measured using commercially available enzyme-linked immunosorbent assay (ELISA) kits (Abcam) according to the manufacturer's instructions

Oral glucose tolerance test

Blood samples from tail vein were collected in fasted animals and 15, 30, 60, 120, and 180 min after oral glucose administration in a dose of 3 g/kg. Blood glucose was measure by using glucometer AccuChek (Roche, Germany).

Insulin tolerance test

Fasted animals received intravenous injection of insulin in a dose of 0.75 U/kg body weight. Glucose concentration was measured in blood obtained from the tail vein at 0, 15, 30, 45, 60, and 90 min after insulin injection with the use of AccuChek glucometer.

Plasma insulin and glucose concentration

Plasma glucose concentration was measured using AccuChek glucometer. Plasma insulin concentration was determined with an ELISA insulin assay (Rat/Mouse Insulin, Millipore, Burlington, MA, USA).

HOMA-IR

The HOMA-IR index value was calculated according to the following formula [30]:

$$HOMA-IR = [\text{fasting glucose (mg/dL)} \times \text{fasting insulin (lU/mL)}]/2430$$

Protein concentration

Protein concentration in tissue homogenates was measured with the bicinchoninic acid protein assay kit (Sigma-Aldrich, St. Louis, MO, USA). Bovine serum albumin (FFA, Sigma-Aldrich) was used as a standard.

Statistical significance estimation and correlation analysis

Statistical significance between experimental groups was estimated using analysis of variance with Tukey honestly significant difference post hoc test for unequal n numbers. Significance level was set to $P < 0.05$. Pearson's r approach with Bonferroni correction for multiple comparisons was used to establish relationships between selected variables. For adipokine and insulin sensitivity parameters, the Pearson's r P-value vas adjusted to 0.002 (25 correlations). For adipokine and individual molecular species of adipose tissue lipids, Pearson's r P-value was adjusted to 0.0002 (249 correlations).

Results

HOMA-IR, oral glucose tolerance test, and ITT

The HOMA-IR index increased in the HFD group by 93% ($P < 0.05$) compared with the control group. Animals fed an HFD developed IR, as evidenced by elevated fasting blood glucose concentration, impaired glucose tolerance, reduced insulin responsiveness, and increased HOMA-IR index. Metformin normalized insulin-related parameters to control values (Table 1; Fig. 1).

Plasma adiponectin and TNF-α concentration

Plasma adiponectin concentration significantly decreased in the HFD group compared with the control group ($P < 0.05$). Metformin treatment caused an elevation of adiponectin compared with the HFD group but was still lower than in the control group ($P < 0.05$). Plasma TNF-α concentration increased in the HFD group compared with control group ($P < 0.05$), whereas metformin treatment restored the content of TNF-α to control value (Table 1).

Table 1
Metabolic parameters and plasma FFA concentration in rats with HFD-induced insulin resistance and under the HFD and Met treatment.

Metabolic parametes and plasma FFA concentration	Control	HFD	HFD/Met
Fasting plasma glucose concentration (mg/dL)	96.8 ± 14.1	141.3 ± 22.9*	103.6 ± 6.3†
Fasting insulin concentration (μU/mL)	50.5 ± 10.2	66.7 ± 7.8*	49.2 ± 14.6†
HOMA-IR	2.00 ± 0.5	3.87 ± 0.68*	2.10 ± 0.64†
Plasma adiponectin concentration (μg/mL)	19.4 ± 2.9	11.2 ± 1.4*	16.4 ± 2.7*,†
Plasma TNF-α concentration (ng/mL)	1.57 ± 0.19	2.67 ± 0.49*	1.57 ± 0.44†
Animal weight (g) in first week of experiment	149.5 ± 4.5	150.62 ± 6.3	149.2 ± 4.8
Animal weight (g) in eighth week of experiment	357.2 ± 35.4	399.6 ± 17	355.2 ± 26.7
Myristic acid (C14:0) [μmol/L]	13.1 ± 2.6	14.6 ± 2.8	14.8 ± 2.7
Palmitoleic acid (C16:1) [μmol/L]	7.4 ± 1.5	2 ± 0.5*	1.9 ± 0.4*
Linoleic acid (C18:2) [μmol/L]	65.7 ± 13.6	58.2 ± 2.2	52.4 ± 9.2*
Palmitic acid (C16:0) [μmol/L]	59.7 ± 10.3	59 ± 2.9	42.7 ± 6.1*,†
Oleic acid (C18:1) [μmol/L]	63 ± 14.6	47.3 ± 8.5*	31.4 ± 6.4*,†
Stearic acid (C18:0) [μmol/L]	33.9 ± 6.7	89.7 ± 11.6*	52.4 ± 8.7*,†
Arachidic acid (C20:0) [μmol/L]	0.96 ± 0.2	4.1 ± 0.8*	2.3 ± 0.4*,†
Behenic acid (C22:0) [μmol/L]	4.8 ± 0.9	11.4 ± 1.2*	10.8 ± 1.9*
Nervonic acid (C24:1) [μmol/L]	1.9 ± 0.2	2.1 ± 0.5	4.2 ± 0.7*,†
Lignoceric acid (C24:0) [μmol/L]	25.0 ± 4.5	67.7 ± 12.3*	46.3 ± 7.3*,†
Total plasma FFA [μmol/L]	275.5 ± 41.8	356.3 ± 21.3*	259.4 ± 16.9†

FFA, free fatty acid; HFD, high-fat diet; HOMA-IR, homeostatic model of assessment with insulin resistance; Met, metformin; TNF, tumor necrosis factor.
Statistics by analysis of variance with Tukey honestly significant difference post hoc test.
*$P < 0.05$ vs control.
†$P < 0.05$ vs HFD.

Plasma FFAs

Total plasma FFA concentration significantly increased in the HFD group ($P < 0.05$) compared with the control group. The highest increase was noticed in long-chain saturated FA: stearic acid (C18:0), arachidic acid (C20:0), and lignoceric acid (C24:0). A reduced content of unsaturated FAs was also observed (palmitoleic acid, C16:1; oleic acid, C18:1). Metformin treatment restored the FFA concentration to control value (Table 1).

Hormone-sensitive lipase pHSLSer563 and pHSLSer660

There were no significant differences in the content of unphosphorylated form of the HSL protein between the three groups in either fat depot. The phosphorylation of the enzyme at both Ser563 and Ser660 residues increased in both types of adipose tissue in the HFD group. In the group fed HFD and treated with metformin, the phosphorylation of HSL decreased at the serine residue (Fig. 2).

Ceramide and DAG concentration

Total content of Cer and DAG significantly increased in both fat depots in the group fed the HFD compared with the control group. Metformin treatment reduced the total content of these lipids compared with the HFD group (for all $P < 0.05$). In VAT, the highest elevation in the HFD group was observed in C18:1-Cer and C18:0-Cer ($P < 0.05$). However, in SAT, the largest increase in Cer content

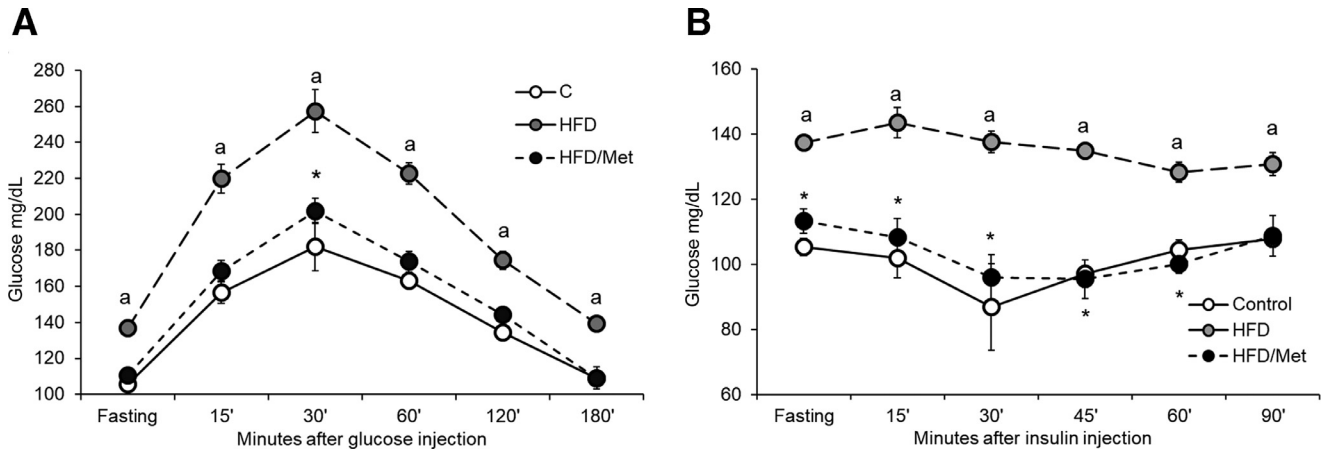

Fig. 1. Treatment with metformin improves glucose and insulin tolerance in animals on a high-fat diet. (**A**) Blood glucose profiles obtained during oral glucose tolerance test. (**B**) Blood glucose profile during intraperitoneal insulin tolerance test. Values are mean ± SD. Statistics by analysis of variance with Tukey honestly significant difference post hoc test. *Statistical significance of $P < 0.05$ versus control group. †Statistical significance of $P < 0.05$ versus HFD group. HFD, high-fat diet; Met, metformin.

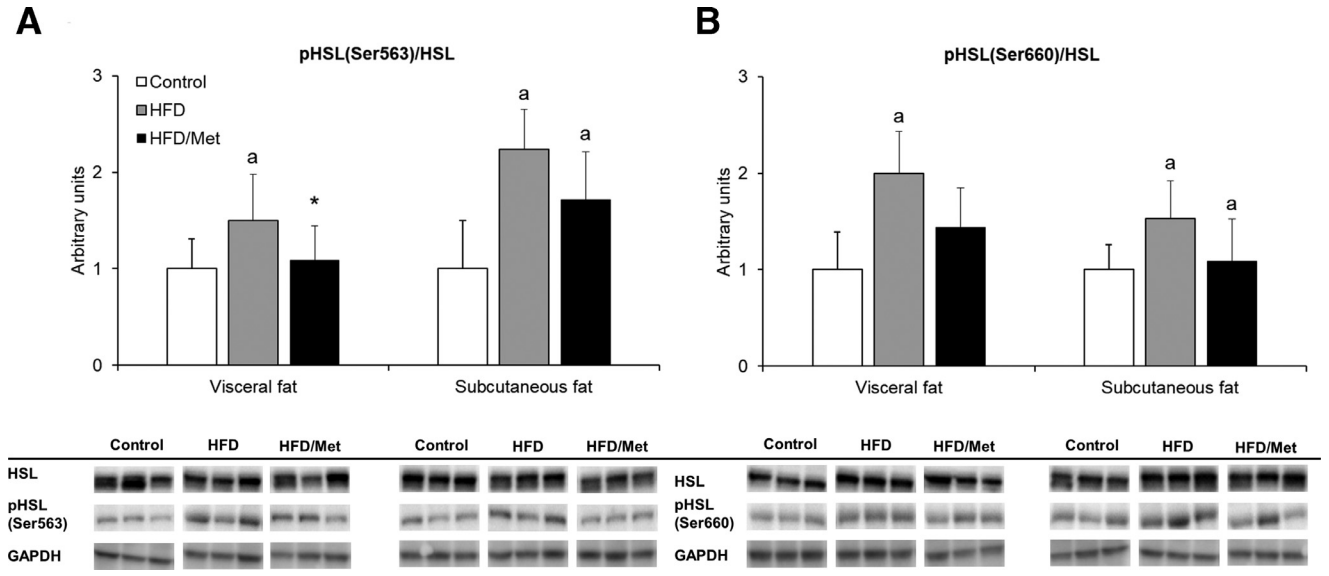

Fig. 2. Protein phosphorylation in insulin signaling pathway. (**A**) Ratio of pHSL (Ser563) to HSL in two depots of adipose tissue. (**B**) Ratio of pHSL (Ser660) to HSL in two depots of adipose tissue, white bars = control group; gray bars = HFD group; black bars = HFD/Met group. Values are mean ± SD. Statistics by analysis of variance with Tukey honestly significant difference post hoc test. *Statistical significance of $P < 0.05$ versus control group. †Statistical significance of $P < 0.05$ versus HFD group. HFD, high-fat diet; HSL, hormone-sensitive lipase; Met, metformin.

caused by an HFD was observed in C18:1-Cer, C22:0-Cer, and C24:0-Cer. In the HFD group given metformin, the level of all Cers in both fat depots was significantly lower than in the HFD group, with the exception of C24:0-Cer in subcutaneous fat, where the level did not differ significantly from its content in the HFD group ($P < 0.05$; Fig. 3; Tables 2 and 3).

In the HFD group, the content of all measured DAG was significantly higher in both depots of adipose tissue compared with the control group ($P < 0.05$). In the group fed HFD and treated with metformin, the content of all DAG was lower than in the HFD group (Fig. 3B; Table 3).

Correlation between Cer and DAG with HOMA-IR, adiponectin, and TNF-α

We found a positive correlation between the HOMA-IR value and visceral fat tissue C16-Cer, C24-Cer, and total Cer content and between HOMA-IR and SAT C18:1-Cer, C22-Cer, and total Cer level. Moreover, VAT Cer (C16-Cer and total Cer) positively correlated with the plasma TNF-α concentration. Cytokines also positively correlated with Cer in subcutaneous fat tissue (C18:1-Cer, C18-Cer, and total Cer). Negative correlations were observed between plasma adiponectin and different Cer species from both depots. More precisely, in visceral fat tissue, adiponectin was strongly correlated with C16-Cer, C18:1-Cer, C18-Cer, C20-Cer, and total Cer. In subcutaneous fat tissue, adiponectin was mainly correlated with C16-Cer, C18:1-Cer, C22-Cer, and total Cer (Table 4).

We also observed a strong correlation between the HOMA-IR value and the DAG content from both fat depots. All measured DAG in VAT (except 18/18:1) strongly correlated with HOMA-IR; whereas in SAT, a strong correlation was found with 16/16, 16/18:2, 16/18, and total DAG levels. In addition, all analyzed DAGs from both fat tissues strongly correlated with TNF-α (positively) and with adiponectin (negatively; Table 5).

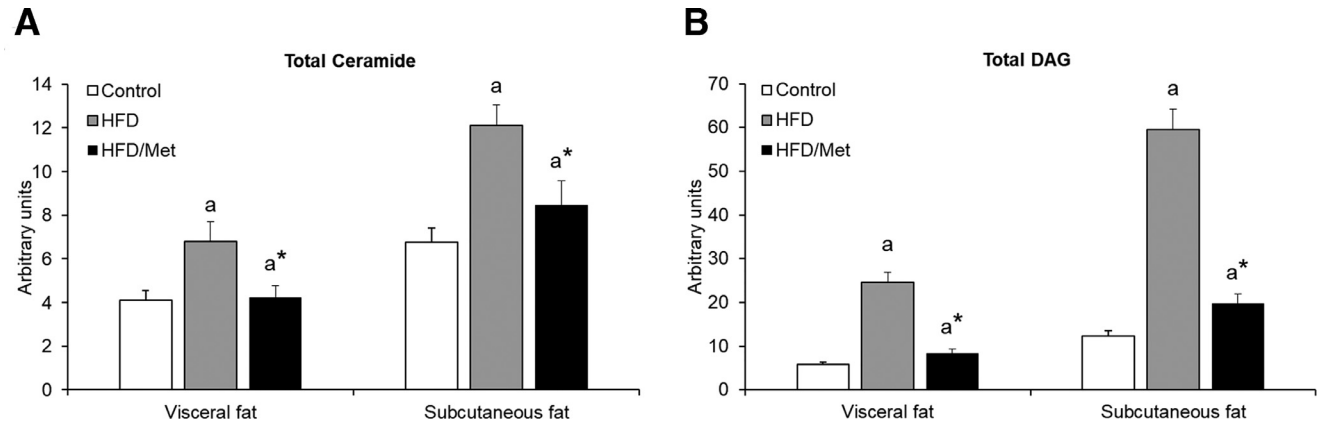

Fig. 3. (**A**) Total ceramide content in two depots of adipose tissue. (**B**) Total DAG content in two depots of adipose tissue; white bars = control group; gray bars = HFD group; black bars = HFD/Met group. Values are mean ± SD. Statistics by analysis of variance with Tukey honestly significant difference post hoc test. *Statistical significance of $P < 0.05$ versus control group. †Statistical significance of $P < 0.05$ versus HFD group. DAG, diacylglycerol; HFD, high-fat diet; Met, metformin.

Table 2
The concentration of individual ceramide molecular species in two depots of adipose tissue

	Visceral fat tissue			Subcutaneous fat tissue		
Cer species	Control	HFD	HFD/Met	Control	HFD	HFD/Met
C14:0-Cer	0.007 ± 0.001	0.015 ± 0.002*	0.013 ± 0.004*,†	0.04 ± 0.006	0.02 ± 0.009*	0.01 ± 0.003*,†
C16:0-Cer	0.97 ± 0.19	1.76 ± 0.27*	1.05 ± 0.19†	2.3 ± 0.35	3.8 ± 0.6*	2.08 ± 0.7†
C18:1-Cer	0.008 ± 0.001	0.03 ± 0.006*	0.01 ± 0.003*,†	0.03 ± 0.007	0.08 ± 0.01*	0.04 ± 0.008†
C18:0-Cer	0.10 ± 0.02	0.53 ± 0.09*	0.38 ± 0.06*,†	0.72 ± 0.08	1.15 ± 0.18*	0.54 ± 0.09*,†
C20:0-Cer	0.09 ± 0.018	0.34 ± 0.08*	0.2 ± 0.04*,†	0.38 ± 0.08	0.56 ± 0.06*	0.24 ± 0.04*,†
C22:0-Cer	0.47 ± 0.08	0.65 ± 0.12*	0.42 ± 0.08†	0.62 ± 0.09	1.3 ± 0.3*	0.75 ± 0.08†
C24:1-Cer	0.54 ± 0.08	0.62 ± 0.09	0.5 ± 0.09†	0.93 ± 0.14	1.25 ± 0.3*	0.99 ± 0.13†
C24:0-Cer	1.92 ± 0.31	2.8 ± 0.42*	1.68 ± 0.3†	1.73 ± 0.33	3.95 ± 0.68*	3.77 ± 0.61*

Cer, ceramide; HFD, high-fat diet; Met, metformin.
Values are mean pmol/mg of tissue.
Statistics by analysis of variance with Tukey honestly significant difference post hoc test.
*$P < 0.05$ vs control.
†$P < 0.05$ vs HFD.

Discussion

Obesity is a complex metabolic state, associated with several disorders, such as atherosclerosis, cardiovascular diseases, IR, and T2D. Although adipose tissue does not play a major role in glucose uptake, it seems to play a dominant one in the pathogenesis of IR. However, the molecular changes in the tissue that initiate these disorders are not completely understood. In the present study, we demonstrated that HFD induced IR, which was manifested by higher fasting plasma glucose and insulin concentration, impaired glucose and insulin tolerance, and higher HOMA-IR values. Metformin treatment enhanced glucose and insulin tolerance and restored the insulin and glucose concentrations to the values observed in the control group. Moreover, as expected, in animals fed an HFD, we observed an increase in plasma FFA concentration, especially the long-chain FAs (Table 2). The elevated FA concentration associated with obesity has been shown frequently by other researches [31–38]. Plasma FFA are taken up by peripheral tissues

Table 3
The concentration of individual DAG molecular species in two depots of adipose tissue.

	Visceral fat tissue			Subcutaneous fat tissue		
DAG species	Control	HFD	HFD/Met	Control	HFD	HFD/Met
16:0/16:0	0.41 ± 0.07	1.1 ± 0.17*	0.44 ± 0.08†	1.04 ± 0.27	3.6 ± 0.62*	0.83 ± 0.09†
16:0/18:1	1.8 ± 0.22	7.2 ± 1.1*	3.17 ± 0.6*,†	4.23 ± 0.78	19.8 ± 3.8*	6.25 ± 0.99*,†
16:0/18:2	1.1 ± 0.20	3.13 ± 0.49*	1.1 ± 0.1†	1.9 ± 0.50	6.4 ± 1*	1.57 ± 0.29†
16:0/18:0	0.29 ± 0.06	1.11 ± 0.18*	0.37 ± 0.07†	0.4 ± 0.08	3.2 ± 0.66*	1.27 ± 0.26*,†
18:1/18:1	1.13 ± 0.25	6.7 ± 0.95*	1.6 ± 0.36†	2.4 ± 0.39	11.1 ± 1.48*	4.89 ± 0.86 *,†
18:1/18:2	1.11 ± 0.20	5.35 ± 0.84*	1.60 ± 0.36†	2.20 ± 0.64	15.2 ± 2.4*	4.80 ± 0.66*,†
18:0/18:1	0.01 ± 0.004	0.05 ± 0.008*	0.017 ± 0.003†	0.03 ± 0.009	0.37 ± 0.066*	0.05 ± 0.01†

DAG, diacylglycerol; HFD, high-fat diet; Met, metformin.
Values are mean pmol/mg of tissue ± SD.
Statistics by analysis of variance with Tukey honestly significant difference post hoc test.
*$P < 0.05$ vs control.
†$P < 0.05$ vs HFD.

Table 4
Relationships between metabolic parameters and the concentrations of individual ceramide species in two fat depots

	Visceral fat tissue			Subcutaneous fat tissue		
Cer species	HOMA-IR	TNF-α	ADIPO	HOMA-IR	TNF-α	ADIPO
C14:0-Cer	0.18	0.48	−0.49	−0.20	−0.087	0.34
	$P = 0.393$	$P = 0.017$	$P = 0.014$	$P = 0.346$	$P = -0.0685$	$P = 0.104$
C16:0-Cer	0.72	0.70	−0.78	0.66	0.67	−0.71
	$P < 0.0002$*	$P < 0.0002$*	$P < 0.0002$*	$P = 0.0003$	$P = 0.0003$	$P < 0.0002$*
C18:1-Cer	0.69	0.69	−0.74	0.69	0.79	−0.79
	$P < 0.0002$*	$P = 0.0003$	$P < 0.0002$*	$P < 0.0002$*	$P < 0.0002$*	$P < 0.0002$*
C18:0-Cer	0.61	0.62	−0.71	0.66	0.77	−0.60
	$P = 0.002$	$P = 0.001$	$P < 0.0002$*	$P < 0.0002$	$P < 0.0002$*	$P = 0.002$
C20:0-Cer	0.64	0.67	−0.74	0.55	0.65	−0.51
	$P = 0.001$	$P = 0.0003$	$P < 0.0002$*	$P = 0.005$	$P = 0.001$	$P = 0.01$
C22:0-Cer	0.49	0.61	−0.50	0.72	0.62	−0.75
	$P = 0.014$	$P = 0.002$	$P = 0.013$	$P < 0.0002$*	$P = 0.001$	$P < 0.0002$*
C24:1-Cer	0.42	0.27	−0.37	0.34	0.58	−0.45
	$P = 0.040$	$P = 0.198$	$P = 0.071$	$P = 0.100$	$P = 0.003$	$P = 0.026$
C24:0-Cer	0.69	0.67	−0.62	0.53	0.37	−0.64
	$P < 0.0002$*	$P = 0.0003$	$P = 0.001$	$P = 0.007$	$P = 0.075$	$P = 0.001$
Total-Cer	0.73	0.72	−0.74	0.74	0.70	−0.82
	$P < 0.0002$*	$P < 0.0002$*	$P < 0.0002$*	$P < 0.0002$*	$P < 0.0002$*	$P < 0.0002$*

ADIPO, adipose; Cer, ceramide; HOMA-IR, homeostatic model of assessment with insulin resistance; TNF, tumor necrosis factor.
Upper values in each cell of the table show Pearson's *r* coefficient, whereas lower values show correlation *P*-value.
*Significant correlations after Bonferroni correction for multiple comparisons.

Table 5
Relationships between metabolic parameters and the concentration of individual DAG molecular species in two fat depots

	Visceral fat tissue			Subcutaneous fat tissue		
DAG species	HOMA-IR	TNF-α	ADIPO	HOMA-IR	TNF-α	ADIPO
16:0/16:0	0.77	0.73	−0.76	0.78	0.77	−0.72
	$P < 0.0002$*	$P < 0.0002$*	$P < 0.0002$*	$P < 0.0002$*	$P < 0.0002$*	$P < 0.0002$*
16:0/18:1	0.74	0.85	−0.78	0.68	0.75	−0.80
	$P < 0.0002$*	$P < 0.0002$*	$P < 0.0002$*	$P = 0.0003$	$P < 0.0002$*	$P < 0.0002$*
16:0/18:2	0.79	0.77	−0.76	0.81	0.81	−0.74
	$P < 0.0002$*	$P < 0.0002$*	$P < 0.0002$*	$P < 0.0002$*	$P < 0.0002$*	$P < 0.0002$*
16:0/18:0	0.74	0.85	−0.76	0.78	0.77	−0.81
	$P < 0.0002$*	$P < 0.0002$*	$P < 0.0002$*	$P < 0.0002$*	$P < 0.0002$*	$P < 0.0002$*
18:1/18:1	0.78	0.78	−0.77	0.63	0.80	−0.78
	$P < 0.0002$*	$P < 0.0002$*	$P < 0.0002$*	$P = 0.0003$	$P < 0.0002$*	$P < 0.0002$*
18:1/18:2	0.75	0.81	−0.80	0.67	0.80	−0.79
	$P < 0.0002$*	$P < 0.0002$*	$P < 0.0002$*	$P = 0.0003$	$P < 0.0002$*	$P < 0.0002$*
18:0/18:1	0.68	0.76	−0.79	0.68	0.84	−0.75
	$P < 0.0002$	$P < 0.0002$*	$P < 0.0002$*	$P = 0.0003$	$P < 0.0002$*	$P < 0.0002$*
Total DAG	0.78	0.82	−0.80	0.72	0.81	−0.81
	$P < 0.0002$*	$P < 0.0002$*	$P < 0.0002$*	$P < 0.0002$*	$P < 0.0002$*	$P < 0.0002$*

ADIPO, adipose; DAG, diacylglycerol; HOMA-IR, homeostatic model of assessment with insulin resistance; TNF, tumor necrosis factor.
Upper values in each cell of the table show Pearson's *r* coefficient, whereas lower values show correlation *P*-value.
*Significant correlations after Bonferroni correction for multiple comparisons.

(e.g., skeletal muscle) where they are used as an energy substrate in the β-oxidation process or as a substrate in de novo lipid biosynthesis. The concentration of plasma FFA depends mainly on the lipolysis of TGs stored in adipocytes, and HSL is the key enzyme responsible for their hydrolysis. It should be emphasized that the activation of HSL is associated with phosphorylation of the enzyme in numerous serine residues, including Ser-660 and Ser-563. Under physiologic conditions, insulin inhibits HSL activity, therefore the release of FFA from TAG is attenuated. However, in the IR state, insulin is not able to effectively inhibit HSL activity, and plasma FFA levels increase. In the present study, we analyzed the phosphorylation state of HSL at activatory sites (Ser-660 and Ser-563) and found that in the HFD group, the HSL phosphorylation increased in both fat depots, which explains the increase in plasma FFA levels. Metformin treatment restored FFA concentration to control value. This effect has been previously observed by other researchers, but the mechanism of this decrease at the adipose tissue level has not been clarified [39–41]. We previously demonstrated that metformin treatment leads to increased FA uptake by skeletal muscles and facilitates their transport to the mitochondria, improving the β-oxidation process, which contributes to a decrease in plasma FFA levels [40]. On the other hand, decreased levels of FAs may result from a reduction in HSL activity, which is manifested by reduced HSL phosphorylation. Metformin is known to activate AMPK [42]. In adipose tissue, activated AMPK phosphorylates the HSL at the Ser-565 residue, preventing phosphorylation at the activatory sites and thus inhibiting the activity of this enzyme [25,26]. In vitro studies have demonstrated that metformin reduces lipolysis in primary adipocytes [43,44]. Consistent with previous reports, we observed reduced phosphorylation of both activation serine residues (Ser-660 and Ser-563), demonstrating that also in vivo, metformin inhibits the lipolytic action of HSL, which is manifested by a decrease in plasma FFA.

As previously mentioned, FAs are a substrate in the de novo synthesis of other lipids, including biologically active lipids (Cer and DAG). It has been demonstrated that accumulation of Cer and

DAG in skeletal muscle is associated with IR [12–14,40,45–47]. However, the effect of adipose tissue bioactive lipids accumulation is poorly understood. There are some papers showing that in obesity, the level of Cer and DAG is increased in subcutaneous fat tissue [20,21,48] and in epicardial fat tissue [21], but there is no information on the role of metformin treatment on the lipid content in adipose tissue. The present study demonstrated that in the group fed the HFD, the content of both Cer and DAG increased in visceral and subcutaneous fat tissues, whereas metformin treatment of animals fed the HFD resulted in a reduction in the content of Cer and DAG in both types of adipose tissues. In addition, it should be emphasized that the reduction of Cer and DAG content was accompanied by a decrease in HSL phosphorylation, which indicates an improvement in the insulin sensitivity of the adipose tissue.

Currently, adipose tissue is perceived not only as a storage for energy in the form of TGs, but also as an endocrine organ that secretes a number of biologically active compounds that affect the insulin sensitivity in peripheral tissues. In the present study, we analyzed the concentration of adiponectin and TNF-α and the correlation between these adipocytokines and individual bioactive lipids in both fat depots. We found that the adiponectin concentration decreased, whereas TNF-α increased in the group fed the HFD. Metformin treatment restored the adipocytokines to control value. In addition, we observed a strong negative correlation between plasma adiponectin concentration and C16-Cer, C18:1-Cer, C18-Cer, and C20-Cer in visceral fat tissue and between plasma adiponectin and C16-Cer, C18:1-Cer, and C22-Cer in subcutaneous fat tissue. Furthermore, we demonstrated a strong negative correlation between plasma adiponectin concentration and content of each measured DAG in both fat tissues. A negative correlation between C16-Cer in SAT and plasma adiponectin was previously demonstrated in women [20]. These results demonstrate that biologically active lipids, Cer, and in particular DAG, are involved in the regulation of the expression or secretion of adipokines from adipose tissue, which means that these lipid species inhibit expression or secretion of adiponectin. Moreover, we observed a strong positive correlation between plasma TNF-α concentration and C16-Cer in VAT and between TNF-α concentration and C18:1-Cer and C18-Cer in subcutaneous fat tissue. Furthermore, a strong positive correlation was observed between TNF-α concentration and all measured DAG species in both visceral and subcutaneous fat tissue. Data presented in the present study indicate that biologically active lipids participate in the regulation of adipocytokines synthesis or secretion from the adipose tissue to the bloodstream.

Taken together, the HFD induced IR, which was manifested by increased insulin and glucose concentration and elevated HOMA-IR value. Moreover, the IR state was associated with increased content of Cer and DAG in both fat depots and decreased plasma adiponectin concentration and increased concentration of TNF-α and FFA. In addition, HFD led to IR of both visceral and subcutaneous fat tissue, which was reflected in the increase of HSL phosphorylation. Metformin treatment restored the IR indicators and FFA concentration to control values. To our knowledge, this is the first time that in vivo metformin has been shown to lead to reductions in both Cer and DAG content in the two fat depots and inhibited the action of HSL, which had a beneficial effect on whole-body insulin sensitivity. Furthermore, we also observed a decrease in plasma TNF-α concentration and an increase in adiponectin concentration in the group treated with metformin. In addition, because we observed a strong correlation between adiponectin (negative) and TNF-α (positive) and the content of bioactive lipids (mainly DAG) in both fat tissues, we postulate that these lipids play an important role in regulating the expression or secretion of adipocytokines.

References

[1] Fernández-Real JM, Ricart W. Insulin resistance and chronic cardiovascular inflammatory syndrome. Endocr Rev 2003;24:278–301.
[2] Yamauchi T, Kamon J, Waki H, Terauchi Y, Kubota N, Hara K, et al. The fat-derived hormone adiponectin reverses insulin resistance associated with both lipoatrophy and obesity. Nat Med 2001;7:941–6.
[3] Engeli S, Gorzelniak K, Kreutz R, Runkel N, Distler A, Sharma AM. Co-expression of renin-angiotensin system genes in human adipose tissue. J Hypertens 1999;17:555–60.
[4] Winkler G, Kiss S, Keszthelyi L, Sápi Z, Ory I, Salamon F, et al. Expression of tumor necrosis factor (TNF)-alpha protein in the subcutaneous and visceral adipose tissue in correlation with adipocyte cell volume, serum TNF-alpha, soluble serum TNF-receptor-2 concentrations and C-peptide level. Eur J Endocrinol 2003;149:129–35.
[5] Scherer PE, Williams S, Fogliano M, Baldini G, Lodish HF. A novel serum protein similar to C1 q, produced exclusively in adipocytes. J Biol Chem 1995;270:26746–9.
[6] Kannel WB. Lipids, diabetes, and coronary heart disease: Insights from the Framingham Study. Am Heart J 1985;110:1100–7.
[7] Larsson B. Obesity, fat distribution and cardiovascular disease. Int J Obes 1991;15(suppl 2):53–7.
[8] Lee MJ, Wu Y, Fried SK. Adipose tissue heterogeneity: implication of depot differences in adipose tissue for obesity complications. Mol Aspects Med 2013;34:1–11.
[9] Khan M, Joseph F. Adipose tissue and adipokines: the association with and application of adipokines in obesity. Scientifica 2014;2014:328592.
[10] Yu C, Chen Y, Cline GW, Zhang D, Zong H, Wang Y, et al. Mechanism by which fatty acids inhibit insulin activation of insulin receptor substrate-1 (IRS-1)-associated phosphatidylinositol 3-kinase activity in muscle. J Biol Chem 2002;277:50230–6.
[11] Shulman GI. Cellular mechanisms of insulin resistance. J Clin Invest 2000;106:171–6.
[12] Straczkowski M, Kowalska I, Nikolajuk A, Dzienis-Straczkowska S, Kinalska I, Baranowski M, et al. Relationship between insulin sensitivity and sphingomyelin signaling pathway in human skeletal muscle. Diabetes 2004;53:1215–21.
[13] Straczkowski M, Kowalska I, Baranowski M, Nikolajuk A, Otziomek E, Zabielski P, et al. Increased skeletal muscle ceramide level in men at risk of developing type 2 diabetes. Diabetologia 2007;50:2366–73.
[14] Straczkowski M, Kowalska I. The role of skeletal muscle sphingolipids in the development of insulin resistance. Rev Diabet Stud 2008;5:13–24.
[15] Turinsky J, O'Sullivan DM, Bayly BP. 1,2-Diacylglycerol and ceramide levels in insulin-resistant tissues of the rat in vivo. J Biol Chem 1990;265:16880–5.
[16] Magkos F, Su X, Bradley D, Fabbrini E, Conte C, Eagon JC, et al. Intrahepatic diacylglycerol content is associated with hepatic insulin resistance in obese subjects. Gastroenterology 2012;142:1444–6. e1442.
[17] Kumashiro N, Erion DM, Zhang D, Kahn M, Beddow SA, Chu X, et al. Cellular mechanism of insulin resistance in nonalcoholic fatty liver disease. Proc Natl Acad Sci U S A 2011;108:16381–5.
[18] Perry RJ, Samuel VT, Petersen KF, Shulman GI. The role of hepatic lipids in hepatic insulin resistance and type 2 diabetes. Nature 2014;510:84–91.
[19] Blachnio-Zabielska AU, Pulka M, Baranowski M, Nikolajuk A, Zabielski P, Gorska M, et al. Ceramide metabolism is affected by obesity and diabetes in human adipose tissue. J Cell Physiol 2012;227:550–7.
[20] Blachnio-Zabielska AU, Koutsari C, Tchkonia T, Jensen MD. Sphingolipid content of human adipose tissue: relationship to adiponectin and insulin resistance. Obesity 2012;20:2341–7.
[21] Błachnio-Zabielska AU, Baranowski M, Hirnle T, Zabielski P, Lewczuk A, Dmitruk I, et al. Increased bioactive lipids content in human subcutaneous and epicardial fat tissue correlates with insulin resistance. Lipids 2012;47:1131–41.
[22] Samad F, Hester KD, Yang G, Hannun YA, Bielawski J. Altered adipose and plasma sphingolipid metabolism in obesity: a potential mechanism for cardiovascular and metabolic risk. Diabetes 2006;55:2579–87.
[23] Samad F, Badeanlou L, Shah C, Yang G. Adipose tissue and ceramide biosynthesis in the pathogenesis of obesity. Adv Exp Med Biol 2011;721:67–86.
[24] Yang G, Badeanlou L, Bielawski J, Roberts AJ, Hannun YA, Samad F. Central role of ceramide biosynthesis in body weight regulation, energy metabolism, and the metabolic syndrome. Am J Physiol Endocrinol Metab 2009;297:E211–24.
[25] Anthonsen MW, Rönnstrand L, Wernstedt C, Degerman E, Holm C. Identification of novel phosphorylation sites in hormone-sensitive lipase that are phosphorylated in response to isoproterenol and govern activation properties in vitro. J Biol Chem 1998;273:215–21.
[26] Daval M, Foufelle F, Ferré P. Functions of AMP-activated protein kinase in adipose tissue. J Physiol 2006;574:55–62.
[27] Persson XM, Blachnio-Zabielska AU, Jensen MD. Rapid measurement of plasma free fatty acid concentration and isotopic enrichment using LC/MS. J Lipid Res 2010;51:2761–5.
[28] Blachnio-Zabielska AU, Persson XM, Koutsari C, Zabielski P, Jensen MD. A liquid chromatography/tandem mass spectrometry method for measuring the in vivo incorporation of plasma free fatty acids into intramyocellular ceramides in humans. Rapid Commun Mass Spectrom 2012;26:1134–40.

[29] Blachnio-Zabielska AU, Zabielski P, Jensen MD. Intramyocellular diacylglycerol concentrations and [U-13 C]palmitate isotopic enrichment measured by LC/MS/MS. J Lipid Res 2013;54:1705–11.
[30] Cacho J, Sevillano J, de Castro J, Herrera E, Ramos MP. Validation of simple indexes to assess insulin sensitivity during pregnancy in Wistar and Sprague-Dawley rats. Am J Physiol Endocrinol Metab 2008;295:E1269–76.
[31] Belfort R, Mandarino L, Kashyap S, Wirfel K, Pratipanawatr T, Berria R, et al. Dose-response effect of elevated plasma free fatty acid on insulin signaling. Diabetes 2005;54:1640–8.
[32] Boden G, Chen X, Ruiz J, White JV, Rossetti L. Mechanisms of fatty acid-induced inhibition of glucose uptake. J Clin Invest 1994;93:2438–46.
[33] Boden G. Role of fatty acids in the pathogenesis of insulin resistance and NIDDM. Diabetes 1997;46:3–10.
[34] Boden G, Lebed B, Schatz M, Homko C, Lemieux S. Effects of acute changes of plasma free fatty acids on intramyocellular fat content and insulin resistance in healthy subjects. Diabetes 2001;50:1612–7.
[35] Boden G, Chen X, Capulong E, Mozzoli M. Effects of free fatty acids on gluconeogenesis and autoregulation of glucose production in type 2 diabetes. Diabetes 2001;50:810–6.
[36] Boden G. Free fatty acids-the link between obesity and insulin resistance. Endocr Pract 2001;7:44–51.
[37] Boden G. Obesity and free fatty acids. Endocrinol Metab Clin North Am 2008;37:635–46. viii-ix.
[38] Itani SI, Ruderman NB, Schmieder F, Boden G. Lipid-induced insulin resistance in human muscle is associated with changes in diacylglycerol, protein kinase C, and IkappaB-alpha. Diabetes 2002;51:2005–11.
[39] Abbasi F, Carantoni M, Chen YD, Reaven GM. Further evidence for a central role of adipose tissue in the antihyperglycemic effect of metformin. Diabetes Care 1998;21:1301–5.
[40] Zabielski P, Chacinska M, Charkiewicz K, Baranowski M, Gorski J, Blachnio-Zabielska AU. Effect of metformin on bioactive lipid metabolism in insulin-resistant muscle. J Endocrinol 2017;233:329–40.
[41] Zabielski P, Hady HR, Chacinska M, Roszczyc K, Gorski J, Blachnio-Zabielska AU. The effect of high fat diet and metformin treatment on liver lipids accumulation and their impact on insulin action. Sci Rep 2018;8:7249.
[42] Meng S, Cao J, He Q, Xiong L, Chang E, Radovick S, et al. Metformin activates AMP-activated protein kinase by promoting formation of the αβγ heterotrimeric complex. J Biol Chem 2015;290:3793–802.
[43] Ren T, He J, Jiang H, Zu L, Pu S, Guo X, et al. Metformin reduces lipolysis in primary rat adipocytes stimulated by tumor necrosis factor-alpha or isoproterenol. J Mol Endocrinol 2006;37:175–83.
[44] Zhang T, He J, Xu C, Zu L, Jiang H, Pu S, et al. Mechanisms of metformin inhibiting lipolytic response to isoproterenol in primary rat adipocytes. J Mol Endocrinol 2009;42:57–66.
[45] Adams JM, Pratipanawatr T, Berria R, Wang E, DeFronzo RA, Sullards MC, et al. Ceramide content is increased in skeletal muscle from obese insulin-resistant humans. Diabetes 2004;53:25–31.
[46] Chavez JA, Summers SA. A ceramide-centric view of insulin resistance. Cell Metab 2012;15:585–94.
[47] Blachnio-Zabielska AU, Chacinska M, Vendelbo MH, Zabielski P. The Crucial Role of C18-Cer in Fat-Induced Skeletal Muscle Insulin Resistance. Cell Physiol Biochem 2016;40:1207–20.
[48] Kolak M, Westerbacka J, Velagapudi VR, Wågsäter D, Yetukuri L, Makkonen J, et al. Adipose tissue inflammation and increased ceramide content characterize subjects with high liver fat content independent of obesity. Diabetes 2007;56:1960–8.